



UNIVERSITÀ
DEGLI STUDI
FIRENZE

FLORE

Repository istituzionale dell'Università degli Studi di Firenze

Different growth factor activation in the right and left ventricles in experimental volume overload

Questa è la Versione finale referata (Post print/Accepted manuscript) della seguente pubblicazione:

Original Citation:

Different growth factor activation in the right and left ventricles in experimental volume overload / P.A. MODESTI; VANNI S; BERTOLOZZI I; CECIONI I; LUMACHI C; PERNA AM; BODDI M; GENSINI GF. - In: HYPERTENSION. - ISSN 0194-911X. - STAMPA. - 43:(2004), pp. 101-108.
[10.1161/01.HYP.0000104720.76179.18]

Availability:

This version is available at: 2158/308454 since:

Published version:

DOI: 10.1161/01.HYP.0000104720.76179.18

Terms of use:

Open Access

La pubblicazione è resa disponibile sotto le norme e i termini della licenza di deposito, secondo quanto stabilito dalla Policy per l'accesso aperto dell'Università degli Studi di Firenze
(<https://www.sba.unifi.it/upload/policy-oa-2016-1.pdf>)

Publisher copyright claim:

(Article begins on next page)

Different Growth Factor Activation in the Right and Left Ventricles in Experimental Volume Overload

Pietro Amedeo Modesti, Simone Vanni, Iacopo Bertolozzi, Iliaria Cecioni, Camilla Lumachi, Avio Maria Perna, Maria Boddi, Gian Franco Gensini

Abstract—Mechanical factors play a key role in activation of cardiac growth factor response in hemodynamic overload, and both cooperate in myocardial remodeling. The present study was performed to investigate whether a different growth factor response is activated in the right and left ventricles in aortocaval fistula and its effects on regional myocardial adaptation. Relations between regional growth factor expression (angiotensin II, insulin-like growth factor-I, and endothelin-1), myocyte shape changes, and collagen deposition were investigated at mRNA and peptide levels in adult pigs after the creation of an aortocaval fistula distal to the renal arteries (n=15) and in sham-operated animals (n=15). The role of angiotensin II was investigated by the administration of angiotensin-converting enzyme inhibitor or angiotensin II receptor antagonist. In the left ventricle, pure volume overload was accompanied by persistent increase of insulin-like growth factor-I mRNA expression, peptide concentration (2.2-fold versus sham at 3 months, $P<0.05$), and significant increase of myocyte length (+29% at 3 months, $P<0.05$). Conversely, the mixed pressure-volume overload faced by the right ventricle resulted in significant regional overexpression of all growth factors investigated (angiotensin II, insulin-like growth factor-I, and endothelin-1), with corresponding increase of myocyte diameter and length and collagen deposition (+117% at 3 months). Collagen accumulation in the right ventricle as well as the increase in right ventricular end-diastolic pressure at the 3-month observation were inhibited by angiotensin II antagonism. The left and right ventricles respond differently to aortocaval fistula, and local growth factor expression is closely related to the regional myocardial adaptation. (*Hypertension*. 2004;43:1-8.)

Key Words: endothelin ■ angiotensin II ■ insulin growth factor ■ hypertrophy ■ ventricular function ■ hemodynamics

Human and experimental studies indicate that a differential pattern of growth factor gene activation is evoked by pressure and volume overload, respectively, with overexpression of angiotensinogen (AGTN), prepro-endothelin-1 (ppET-1), and insulin-like growth factor-I (IGF-I) or isolated activation of IGF-I production.¹⁻³ In the acute phase, growth factor gene expression contributes to maintain left ventricular cardiac function,⁴ whereas in the long term it regulates the pattern of hypertrophy by affecting myocyte growth^{5,6} and collagen deposition.⁷ Increased collagen accumulation characterizes concentric hypertrophy of experimental pressure overload,⁸ whereas no significant changes in fibrillar collagen content have been observed in experimental volume-induced eccentric hypertrophy.^{9,10} The pattern of growth factor gene expression is then finally modified by the transition from hypertrophy to failure with enhanced angiotensin II (Ang II) formation and reduced IGF-I expression.¹¹ Thus, the expression of local growth factors appears to participate in the regulation of the type of cardiac hypertrophy and to characterize the transition to failure.

In aortocaval fistula, the two ventricles are both exposed to increased work load, but experimental studies performed in rats indicate that in addition to volume overload, the right ventricle also faces an increased pressure load caused by the rise in pulmonary systolic pressure,¹²⁻¹⁴ leading to a relative mass increase higher in the right than in the left ventricle.^{2,13} The increased magnitude of right ventricular hypertrophy has also been associated with enhanced collagen accumulation.¹⁵ However, in the large majority of studies on experimental aortocaval fistula, growth factor changes and ventricular function have been investigated only in the left ventricle,¹⁶⁻¹⁸ with no direct comparison of growth factor response in the two different cardiac chambers. Only a single study compared the local expression of IGF-I in the right and left ventricles of rats with aortocaval fistula,² even though IGF-I is not directly involved in myocardial fibrosis. On the other hand, the activation of the renin-angiotensin system (RAS), which conversely is known to directly stimulate both collagen deposition⁷ and overexpression of other fibrogenic growth factors,⁴ has only been investigated through administration of

Received September 15, 2003; first decision October 9, 2003; revision accepted October 23, 2003.

From Clinica Medica Generale e Cardiologia (P.A.M., S.V., I.B., I.C., C.L., M.B., G.F.G.) and the Department of Experimental Surgery (A.M.P.), University of Florence, Florence, Italy.

Correspondence to Prof Pietro Amedeo Modesti, Clinica Medica Generale e Cardiologia, University of Florence, Viale Morgagni 85, 50134 Florence, Italy. E-mail pa.modesti@dfc.unifi.it

© 2003 American Heart Association, Inc.

Hypertension is available at <http://www.hypertensionaha.org>

DOI: 10.1161/01.HYP.0000104720.76179.18

angiotensin-converting enzyme (ACE) inhibitors and angiotensin type 1 (AT1) receptor antagonists, which modified the cardiac load.^{2,15,19} All these experimental studies were performed in rats, which respond to acute volume overload differently from large animals. The high cardiac output in volume-overloaded rats was indeed accomplished solely by increased stroke volume, with no changes in heart rate.¹² In addition, the majority of studies have only investigated the mechanics of the left ventricle,^{16,17} revealing normal indexes of left ventricular function with shortening velocity decreasing only at the terminal stage of heart failure.²⁰ However, the presence of increased hepatic fluid content and ascites at chronic assessment may suggest an approaching right ventricular failure.¹³

Therefore, the present study was designed to compare the hemodynamic adaptations, growth factor (Ang II, ET-1, and IGF-I) expression, and collagen deposition in the right and left ventricles during the development (up to 3 months) of volume overload-induced (aortocaval fistula) myocardial hypertrophy in pigs. In addition, an ACE inhibitor (ramipril) or AT1 receptor antagonist (valsartan) was administered in two groups of animals to investigate the relative role of Ang II on myocardial hypertrophy and collagen deposition in the two ventricles.

Methods

Animals and Study Design

Thirty-six farm pigs of either gender, weighing 38 ± 2 kg, were used in the study. Animals were kept and handled in accordance with the recommendations of the Guide for the Care and Use of Laboratory Animals published by the US National Institutes of Health (NIH Publication No. 85 to 23, Revised 1996). Animals were anesthetized, and volume overload was induced in 15 animals by creating an infrarenal aortocaval fistula (Dacron graft, 8 mm diameter), as previously described,³ whereas 15 animals were sham-operated. At baseline and at 15, 30, 60, and 90 days after surgery, 3 aortocaval-shunted animals and 3 sham-operated animals underwent echocardiographic examination and measurements of hemodynamic parameters. After the pigs were euthanized, the heart was removed, and 2 transmural left and right ventricular free wall specimens, taken midway from base to apex, were immediately placed in liquid nitrogen for measurement of ET-1, IGF-I, Ang II, and hydroxyproline cardiac content and for RT-PCR studies and in 10% formalin solution for myocyte morphometry.

Three days after surgery, 6 operated animals were randomized to treatments with ACE inhibitor (ramipril, 5 mg per day; $n=3$) or AT1 receptor antagonist (valsartan, 80 mg daily orally; $n=3$), and treatments were continued for 3 months. The doses of valsartan and ramipril were preliminarily checked to reduce (60% to 40% inhibition at 3 and 24 hours, respectively) the increase in mean arterial pressure after Ang II or Ang I infusion, respectively, without causing any significant effect on resting blood pressure.⁴

Ventricular Function and Hemodynamic Measurements

Two 6F pigtail catheters were introduced into the left femoral artery and advanced to monitor left ventricular pressure. A pulmonary artery catheter was used to measure capillary wedge pressure (PCWP), pulmonary artery pressure (PAP), right atrial pressure (RAP), cardiac output (CO), and cardiac index (CI). Echocardiographic measurements were taken according to the recommendations of the American Society of Echocardiography²¹; left ventricular mass indexed by body weight (LVMI), left ventricular volumes (v), and left ventricular meridional wall stresses were calculated by means of standard formulas, as previously reported.⁴ Left ventricular

TABLE 1. GAPDH, AGTN, ppET-1, and IGF-I Primers for RT-PCR

Primers	Sequence 5'—3'	cdNA Sizes, bp
GAPDH	5'TGAAGGTCGGAGTCAACGGA	987
	3'CATGTGGCCATGAGGTCCA	
AGTN	5'CTGCAAGGATCTTATGACCT	238
	3'TACACAGCAAACAGGAATGG	
ppET-1	5'GTCAACACTCCCGAGCAGCTT	304
	3'CTGGTTTGTCTTAGGTGTCCTC	
IGF-I	5'ACATCTCCATCTCTGGATTTCTTTTGC	510
	3'CCCTCTACTTGCCTTCTCAATGTACTTCC	

GAPDH indicates glyceraldehyde-3-phosphate dehydrogenase; AGTN, angiotensinogen; ppET-1, prepro-endothelin-1; and IGF-I, insulin-like growth factor-I.

stroke work index was calculated as $LVSWI = (\text{mean AoP} - \text{PCWP}) \times \text{SVI}$, where AoP is aortic pressure and SVI is stroke volume index, which equals CI divided by heart rate.

Right ventricular stroke work index (RVSWI) was calculated as²² $RVSWI = (\text{mean PAP} - \text{mean RAP}) \times \text{SVI}$.

Measurements were analyzed independently by two experienced echocardiographers. Interobserver and intra-observer variabilities were $4.1 \pm 0.5\%$ and $2.5 \pm 0.3\%$ for cavity size and $3.7 \pm 0.4\%$ and $2.1 \pm 0.3\%$ for wall thickness, respectively.

Quantification of Growth Factor mRNA and Peptide Levels in Myocardium

Myocardial levels of ppET-1, AGTN, and IGF-I transcripts were quantified by RT-PCR with glyceraldehyde-3-phosphate dehydrogenase (GAPDH) as internal standard, using specific primers (Table 1), as previously reported.¹

Measurements of Ang II concentration in myocardial tissue were performed by RIA assay after preliminary acid-alcohol extraction and concentration on Sep-Pak cartridges for HPLC separation as previously described.⁴ Cardiac ET-1 was determined by specific RIA assay according to Wei et al.²³ IGF-I was assayed with RIA in homogenated tissue according to Jalil et al.²⁴

Myocardial Collagen Content and Myocyte Morphometry

Myocardial collagen concentrations were measured by the hydroxyproline assay according to Woessner.²⁵ To measure myocyte and sarcomere lengths, the myocytes were isolated from formalin-fixed tissue by means of the potassium hydroxide digestion method, according to Tamura et al.²⁶ Briefly, small pieces of formalin-fixed tissue were rinsed in PBS and put into 12.5 mol/L KOH solution for 24 hours. Rod cells were then separated by filtration through nylon mesh (250 μm).

Statistical Analysis

Data are expressed as mean \pm SD. Comparisons were performed by means of 1-way ANOVA and the Student t test, followed by the Tukey multiple-range comparison test, as appropriate. Linear relations were analyzed with the Pearson correlation, with the use of BMDP statistical software (BMDP Statistical Software Inc).

An expanded Methods section can be found in an online supplement available at <http://www.hypertensionaha.org>.

Results

Hemodynamic Changes

The fistula remained pervious in all experimental animals, and no animal showed signs of heart failure or ascites during the study. In operated animals, LVMI was 2.1-fold versus

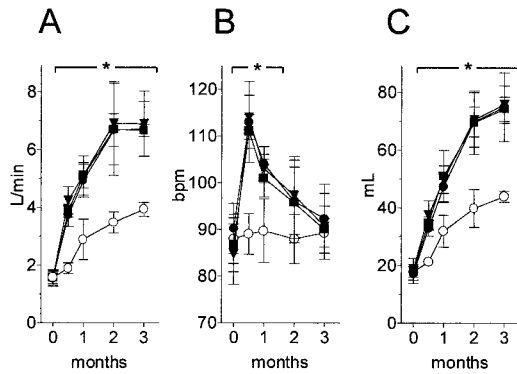


Figure 1. Cardiac output (A), heart rate (B), and stroke volume (C) in pigs with aortocaval fistula treated with placebo (●; n=15), ramipril (▲; n=3), or valsartan (△; n=3) and in sham-operated animals (○; n=15). Each point at different experimental times represents mean±SD of 3 pigs. Values obtained at each experimental time in shunted animals are compared with both baseline values measured in the same pig and values measured at the same experimental time in 3 sham-operated pigs. * $P<0.05$ vs baseline and vs sham.

sham at 3 months (from 2.1 ± 0.5 g/kg to 4.3 ± 0.5 g/kg, $P<0.001$).

As a consequence of the creation of an aortocaval fistula, total peripheral resistance significantly decreased and CO

significantly increased, remaining high versus sham at all experimental times (Figure 1A and Table 2). Heart rate increased after surgery but returned to baseline levels at 2 months (Figure 1B). The high CO then was accomplished solely by the increase in stroke volume (Figure 1C).

Right ventricular pressure significantly increased after surgery, whereas left ventricular pressure remained unchanged (Figure 2). As a consequence, the RVSWI showed a larger increase than the LVSWI (+216% and +70% versus baseline at 2 weeks, respectively) (Figure 2). At all the following observation times, the LVSWI remained almost steady (Figure 2). The left ventricular end-systolic stress (ESS) was nonsignificantly different versus sham at all experimental times, and the preload-independent index ESS/end-systolic volume index (ESVI) ratio remained significantly reduced versus sham at all the experimental times (Table 2), thus indicating a persistent normal left ventricular contractile function. Conversely, the end-diastolic right ventricular pressure significantly increased at the 3-month observation versus values measured at 2 months, concomitant with a significant reduction of the RVSWI (Figure 2).

The development of left ventricular hypertrophy as well as the hemodynamic changes induced by aortocaval fistula were not affected by the Ang II antagonist (Figure 1). However,

TABLE 2. Hemodynamic Changes Following the Creation of Aortocaval Fistula

	Baseline	2 Weeks	1 Month	2 Months	3 Months
Shunt					
LVEDD, mm	23±1	26±2*	29±2*	31±2*	34±1*
LVEDD, mm	35±2	42±1*	45±1*	51±1*	55±2*
SWT, mm	11.8±1.2	12.3±0.4*	13.1±0.2*	12.9±0.5*	14.0±0.8*
DWT, mm	7.3±0.5	6.8±0.7	9.0±0.6*	9.7±0.5*	10.0±0.8*
LVMI, g/kg	2.11±0.45	3.20±0.10*	3.42±0.30*	3.82±0.21*	4.32±0.53*
PVR, mm Hg · mL ⁻¹ · min · kg	1.96±0.50	0.75±0.04*	0.74±0.10*	0.73±0.11*	0.81±0.13*
LVEDP, mm Hg	7.7±2.6	9.8±1.3	10.0±0.6	9.0±1.3	11.0±4.9
RVEDP, mm Hg	6.8±2.8	10.0±0.9*	10.8±1.0*	11.5±0.5*	19.6±2.6*†
ESS, kdyne/cm ²	47±8	52±5	56±4	60±5	66±3
ESS/ESVI	163±27	134±7*	131±18*	153±9*	137±7*
EF, %	60±6	68±4	68±5	72±3	67±5
Sham					
LVEDD, mm	23±2	23±2	24±1	26±1	27±1
LVEDD, mm	34±2	35±1	37±2	39±2	42±1
SWT, mm	10.7±0.6	10.8±0.8	11.3±0.8	11.5±0.5	11.7±0.6
DWT, mm	7.3±0.6	7.2±0.3	7.2±0.3	7.7±0.3	8.2±0.3
LVMI, g/kg	2.06±0.22	1.98±0.12	2.07±0.28	1.86±0.26	1.98±0.19
PVR, mm Hg · mL ⁻¹ · min · kg	1.77±0.31	1.61±0.31	1.21±0.29	1.33±0.14	1.38±0.05
LVEDP, mm Hg	7.3±4.2	7.0±3.6	7.7±2.9	7.0±2.6	6.3±2.5
RVEDP, mm Hg	4.3±1.5	5.0±1.7	4.0±0.1	5.0±0.1	5.3±0.6
ESS, kdyne/cm ²	53±8	54±9	54±7	56±5	58±6
ESS/ESVI	179±29	180±20	156±11	189±13	193±21
EF, %	62±2	64±4	67±5	68±3	67±3

Values are mean±SD. DWT indicates diastolic wall thickness; EF, ejection fraction; ESS, end-systolic stress; ESVI, end-systolic volume index; LVEDD left ventricular end-diastolic diameter; LVEDP left ventricular end-diastolic pressure; LVESD, left ventricular end-systolic diameter; LVMI, left ventricular mass index; PVR, peripheral vascular resistance; RVEDP right ventricular end-diastolic pressure; and SWT, systolic wall thickness.

* $P<0.05$ vs sham; † $P<0.05$ vs 2 months.

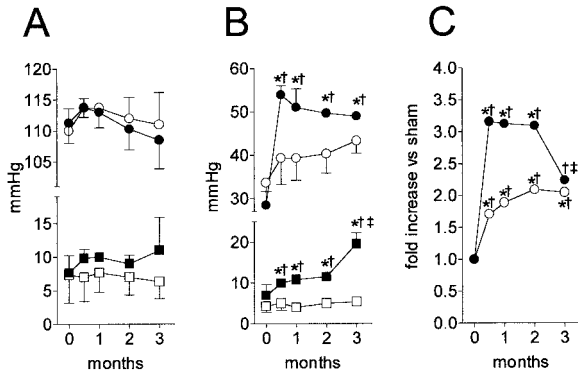


Figure 2. Left (A) and right (B) ventricular systolic (circles) and diastolic (squares) pressure in volume-overloaded (filled symbols) and sham-operated animals (empty symbols). C, Changes in right ventricular (●) and left ventricular (○) stroke work index induced by aortocaval fistula versus sham. Each point at different experimental times represents mean±SD of 3 pigs. Values obtained at each experimental time in shunted animals are compared with both baseline values measured in the same pig and values measured at the same experimental time in 3 sham-operated pigs. **P*<0.05 vs baseline; †*P*<0.05 vs sham; ‡*P*<0.05 vs values measured at 2 months.

both ACE inhibitor (ramipril) and AT1 antagonist (valsartan) blunted the final increase (3-month) of the end-diastolic right ventricular pressure detectable in untreated animals with aortocaval fistula (11.2±1.9 and 10.5±1.3 mm Hg in ACE- and AT1-blocked animals, *P*<0.05 versus untreated animals).

Myocardial Collagen and Morphometry

Three months after application of the aortocaval fistula, the collagen concentration in the right ventricle was 2-fold versus sham (+117%), with only a minor increase (+29%) in the left ventricle (Figure 3). The long-term administration of AT1 antagonist to animals with an aortocaval fistula significantly reduced collagen deposition in the right ventricle (−37% versus placebo, *P*<0.01), whereas no changes were observed in the left ventricle (Figure 3). Conversely, ACE inhibition reduced collagen concentration in the myocardial tissue of both the right and the left ventricles (−58% and −35%, respectively, *P*<0.05 for both versus placebo).

The length of cardiomyocytes was significantly increased versus sham at 1 month in both ventricles (Figure 4). Myocytes isolated from the left ventricle showed progressive

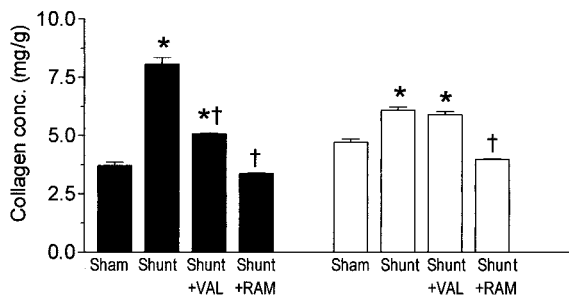


Figure 3. Collagen concentration at 3 months after surgery in right (filled bars) and left (open bars) ventricular myocardium of sham-operated animals and of shunted pigs treated with placebo, valsartan, or ramipril. Each bar represents mean±SD of 3 pigs. **P*<0.05 vs sham; †*P*<0.05 vs placebo.

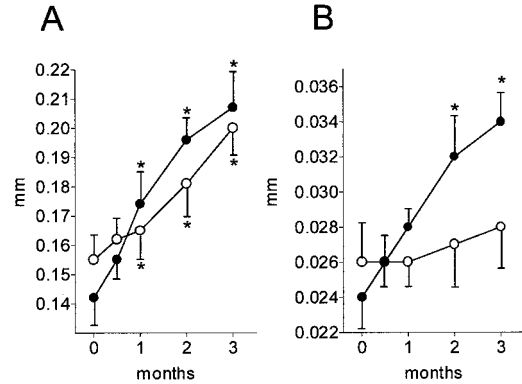


Figure 4. Length (A) and diameter (B) of myocytes isolated from the left ventricle (○) and right ventricle (●) of shunted pigs. Each point at different experimental times represents mean±SD of 3 pigs. Values obtained at each experimental time are compared with values obtained in sham-operated animals. **P*<0.05 vs sham.

elongation up to the last experimental time, whereas the length increase in right ventricular myocytes did not progress further from the second to the third month (Figure 4). In addition, different from left ventricular myocytes, right ventricular myocytes showed a significant increase in cell transverse size at 2 and 3 months versus sham (Figure 4). The creation of an aortocaval fistula did not modify sarcomere length either in the left ventricle (1.97±0.09 and 1.96±0.08 μm in sham and shunted pigs at 3 months, respectively) or in the right ventricle (2.08±0.05 and 2.06±0.08 μm). The rate of cardiomyocyte growth was unaffected by ACE inhibitor and AT1 antagonist administration.

Growth Factor Production

In overloaded right ventricles of animals with aortocaval fistula, both the AGTN and ppET-1 genes were markedly activated (Figure 5). The AGTN/GAPDH mRNA ratio was 3.5-fold versus sham at 2 weeks, and the ppET-1 gene was 9.3-fold versus sham after 1 month. Both transcripts remained overexpressed at the following observation periods (4.1-fold and 7.8-fold versus sham at 3 months, respectively). Conversely, both the AGTN and the ppET-1 genes in the left ventricle were unaffected by volume overload (Figure 5). The selective increase of both Ang II and ET-1 formation in the right ventricle of animals with aortocaval fistula was confirmed by radioimmunological assays at the peptide level (Figure 6). At univariate analysis, myocardial ET-1 concentration was positively related to myocyte diameter (*r*=0.49, *P*<0.01)

The IGF-I mRNA expression in the myocardial tissue was conversely enhanced both in the right and in left ventricles at 1 month and remained overexpressed at 2 months (Figure 5 and Figure 6). Then, at 3 months, IGF-I mRNA expression and peptide concentration further increased in the left ventricle versus values measured at 2 months, whereas in the right ventricle IGF-I mRNA expression and peptide concentration showed a sharp reduction (Figure 5 and Figure 6). Univariate analysis revealed that regional IGF-I myocardial concentration was related to both SWI (*r*=0.74 and *r*=0.55 in the right

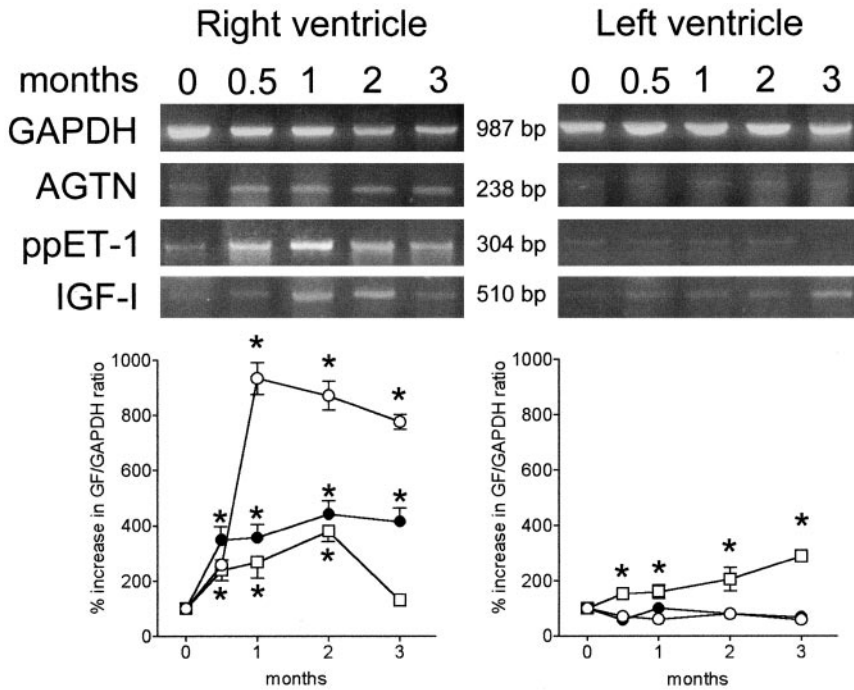


Figure 5. Expression of GAPDH, AGTN, ppET-1, and IGF-I mRNAs in the right ventricle (left panel) and left ventricle (right panel) of volume-overloaded pigs. Top panels: Representative RT-PCR experiment. Bottom panels: Percent increase in densitometric ratio to GAPDH for AGTN (●), ppET-1 (○), and IGF-I (□) in shunted animals. Each point at different experimental times represents mean±SD of values measured in 3 volume-overloaded pigs. **P*<0.05 vs sham.

and the left ventricle, respectively, *P*<0.05 for both) and myocyte length (*r*=0.50, *P*<0.05).

AT1 antagonism significantly reduced the myocardial concentration of Ang II in the right ventricle (38±9 pg/g versus 64±10 pg/g in treated and untreated animals, respectively, *P*<0.05) and a complete normalization was induced by ACE inhibition (25±8 pg/g, NS versus sham) (Figure 6). Both valsartan and ramipril significantly reduced the ET-1 concentration in the right ventricle (Figure 6). Conversely, IGF-I myocardial concentration in the right ventricle was increased by both ACE inhibition and AT1 antagonism (Figure 6).

Discussion

The main findings of the present study are that in chronic aortocaval shunt (1) the different experimental mechanical load and geometry of the two ventricles induce a distinct regional pattern of activation of cardiac growth factors, with overexpression of AGTN and ppET-1 genes restricted to the right ventricular myocardium (facing both pressure and volume overload) and IGF-I gene expression activated in both ventricles; (2) the different patterns of growth factor expression selectively regulate the adaptation of myocyte shape to mechanical load (IGF-I for cell length and ppET-1 for cell

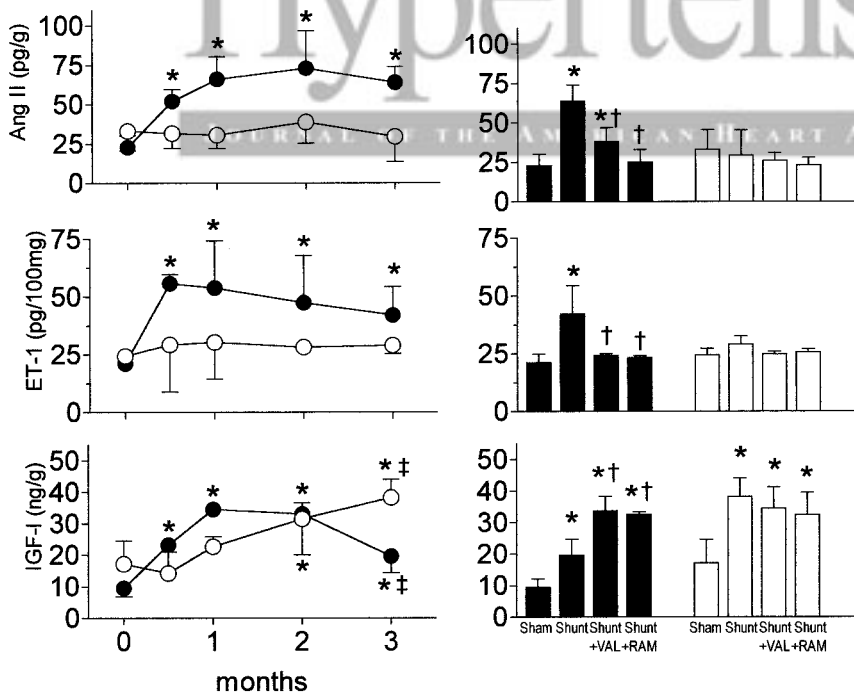


Figure 6. Left panels: Concentrations of Ang II, ET-1, and IGF-I in myocardial tissue of the right ventricle (●) and left ventricle (○) of pigs with aortocaval fistula. Right panels: Effect of AT1 antagonism and ACE inhibition on myocardial concentration of Ang II, ET-1, and IGF-I in the right ventricle (filled bars) and left ventricle (empty bars) of pigs with aortocaval fistula. Each point at different experimental times represents mean±SD of 3 pigs. **P*<0.05 vs sham; †*P*<0.05 vs placebo; ‡*P*<0.05 vs 2 months.

diameter increase) and affect collagen deposition (AGTN and ppET-1); (3) a reduction of IGF-I production in the right ventricle at 3 months occurred simultaneously with increased right ventricular end-diastolic pressure.

Hemodynamic and Cardiac Adaptations to Aortocaval Fistula

In our animals, the creation of an aortocaval shunt caused a persistent 2.4-fold increase in CO versus sham-operated animals, resulting in a 2.1-fold increase of LVMI at 3 months, in agreement with previous studies.^{2,13,27,28} Unlike in rats,¹² our pigs had CO that was mainly sustained by heart rate during the first month. Only at 2 and 3 months after surgery did dilation of the cardiac chamber cause CO to be chronically maintained by increased stroke volume, because heart rate returned to baseline. Investigation of cell morphometry offers further insight into the mechanism of cardiac adaptation in large mammals. We used the potassium hydroxide digestion method to obtain high-quality data on cell and sarcomere length not otherwise possible with standard tissue sectioning methods. The constant midwall sarcomere length, also observed in dogs with severe volume overload induced by arteriovenous shunt,²⁹ clearly indicates that the chronic cardiac adaptation to severe volume overloading does not utilize the Frank-Starling mechanism. The pattern of adaptation is rather related to the progressive addition of new sarcomeres (11 and 8 per month in the right ventricle and left ventricle, respectively). Indeed the final increase in myocyte length, which became significant at 1 month after surgery, accounts for most of the 45% to 50% increase in the left ventricular chamber circumference at 3 months.

Although in isolated myocytes the cell diameter data probably represent major diameters and may not truly represent overall changes in transverse myocyte size, cell morphometry showed a different myocyte adaptation to aortocaval fistula in the two ventricles because notwithstanding the length of both right and left ventricular myocytes was increased, only right ventricular myocytes showed a progressive increase in cell diameter at subsequent observations. However, the 63% increase in right ventricular systolic pressure indicates that in agreement with previous studies,^{12,28} the right ventricle in aortocaval fistula faces a mixed pressure-volume overload, whereas the left ventricle faces a pure volume overload with a selective increase in diastolic stress.^{2,12,14,30} As a consequence, the acute stroke work increase was 3.1-fold higher in the right than in the left ventricle after the creation of an aortocaval fistula.

In our experimental model, the left ventricular hypertrophy at 3 months was compensatory, as the ESS/ESVI ratio, an index used to investigate left ventricular contractile function in volume overload,³¹ did not increase. The complex geometry of the right chamber makes difficult the calculation of right ventricular wall stresses.³² However, the right ventricular performance, expressed by RVSWI, was reduced at 3 months versus values measured at 2 months. The approach of a right ventricular dysfunction at 3 months was also indicated by the contemporary 70% increase in end-diastolic pressure versus values measured at 2 months.

The factors responsible for the adaptation of myocyte shape and ventricular function to the different mechanical load are poorly understood, but the present study offers relevant insights into the possible role of regional growth factor expression.

Differential Activation of Growth Factors in the Right and Left Ventricles

One of the main findings of the present study is that the different mechanical loads faced by the two ventricles in aortocaval fistula induce distinct regional growth factor gene activation, with overexpression of AGTN, ppET-1, and IGF-I in the right ventricle and isolated overexpression of IGF-I in the left ventricle. Growth factor overexpression in the right ventricle exposed to a mixed pressure-volume overload persists during the chronic phase. Previous studies showed that in pressure-overloaded left ventricles, the overexpression of AGTN and ppET-1 soon recedes (within 24 hours) when the ESS is normalized.³ The different mechanical properties of the right and the left ventricular walls might be responsible for the persistent enhancement of AGTN and ppET-1 gene expression observed in the present study. Indeed, notwithstanding the fact that the pressure increase faced by the right ventricle of volume-overloaded pigs (+26 mm Hg) was lower than the pressure increase applied to the left ventricle of aortic-banded pigs in the previous study (+60 mm Hg), the percent pressure increases versus baseline levels were similar (+63% and +50% respectively). Therefore, because of its thin wall, the right ventricle might be unable to normalize wall stress.

In our animals, a close relation was observed between the cardiac expression of IGF-I and mechanical load, as also revealed in patients with aortic valve disease,¹ and healthy athletes.³³ Also for IGF-I, the regional cardiac formation appears to be elicited by the stretching of the single myocyte rather than by the absolute mechanical load applied to the ventricle, as also reported in skeletal muscle fibers.³⁴ Indeed, during the early period after the application of aortocaval fistula, cardiac IGF-I production was prevalent in the right ventricle, even though it faces an absolute work load lower than that of the left myocardium. The mechanical characteristics of the ventricular wall may therefore determine the profile of growth factor gene expression.

Activated Growth Factors and Ventricular Adaptation to Increased Work Load

The IGF-I, overexpressed in both the right and left ventricles, appears to play a key role in sustaining myocyte adaptation to volume overload. In isolated myocytes, IGF-I has been reported to induce the "in series" apposition of new sarcomeres.³⁵ In the present study, IGF-I was positively related to myocyte elongation, a change that determines the final adaptation of ventricles to volume overload. On the other hand, ET-1 was positively related to myocyte transverse size. ET-1 has indeed been reported to induce myocyte growth with "in parallel" apposition of new contractile elements.³⁶

Administration of Ang II antagonists indicates that Ang II plays a minor role in myocardial hypertrophy induced by aortocaval fistula. Neither AT1 receptor nor ACE inhibition

affected the development of left ventricular hypertrophy. This appears to be in contrast to previous findings in small animals.^{19,37} However, different from the quoted studies, we used drug doses that counteract Ang I-induced or Ang II-induced pressure increases but did not affect baseline blood pressure. Therefore, the dose used was adequate to block the AT1 receptor and cardiac ACE but did not affect mechanical load. In addition, in agreement with previous studies,³⁸ a reduction of myocardial Ang II was indeed found in animals assigned to ACE inhibition. Therefore, the present experiments argue against a direct involvement of RAS in the development of cardiac hypertrophy in aortocaval fistula.

According to the present data, Ang II appears to play a primary role in collagen deposition. A selective increase in collagen concentration in the right myocardium was previously observed in small animals with aortocaval fistula^{9,10,15} and in human congenital heart disease with mixed pressure and volume right ventricular overload.³⁹ However, because of the treatment protocol and the difficulty to perform accurate dose findings in small animals, previous studies failed to observe changes in cardiac collagen in animals treated with Ang II antagonists. In our animals, AT1 blockade reduced collagen deposition in the right ventricle. AT1 receptors, which are the prevalent receptor subtype in isolated fibroblasts, are known to stimulate collagen synthesis.^{40,41} The present data do not allow us to exclude that Ang II binding to unblocked AT2 receptors might participate in the inhibition of collagen synthesis, as previously hypothesized.⁴² On the other hand, an even larger inhibition of collagen deposition was found in the animals treated with the ACE inhibitors when compared with the group allocated to the AT1 antagonist. Although a definitive clarification of the importance of bradykinin would require further study with direct measurement of the bradykinin levels, the beneficial effect of the ACE inhibitor-mediated potentiation of the kinin system may be at least hypothesized.^{43,44}

Ang II inhibition also limited the reduction of IGF-I in the right ventricle, and this effect might be related to the reduced collagen deposition. IGF-I synthesis can be activated by either sympathetic activity through extracellular signal regulated kinase-mediated activation of GATA4⁴⁵ and through mechanical stretching.^{46,47} The prevalent IGF-I expression in the right ventricular myocardium in the presence of a common exposition to sympathetic system overactivity suggests a prevalent role for the mechanical stimulus. Enhanced collagen accumulation in the right ventricle might thus limit myocyte stretching by reducing the sensitivity of myocyte mechanosensors and contributing to the decline of the right ventricular IGF-I formation observed at 3 months. Collagen deposition might thus affect cardiac function, not only by impairing cardiac compliance but also by limiting the enhancement of IGF-I formation. A reduction of IGF-I cardiac production concurrently with the impairment of left ventricular function has previously been observed in patients with aortic valve disease¹ and in experimental animals.⁴⁸ According to the present findings, IGF-I expression might also play a role in supporting right ventricular function, as indicated by the close relation between regional IGF-I peptide level and right ventricular performance expressed by RVSWI. The

clinical mark of reduced IGF-I production was the increase in end-diastolic pressure. Indeed, the reduced IGF-I overexpression in the right ventricle at 3 months versus values measured at 2 months occurred simultaneously with the reduction of RVSWI and with the contemporary increase in end-diastolic pressure. The measurement of peptide concentration in myocardial tissue confirmed that both gene transcription and peptide myocardial concentration reduce with increased diastolic pressure. The relation among collagen deposition, impaired IGF-I cardiac production, and reduced function is further stressed by the effect of Ang II inhibition.

In conclusion, the present study indicates that the interaction between the characteristics of the ventricular wall and the mechanical load is a determinant for local cardiac growth factor expression, which regulates the adaptation of myocyte shape and interstitial matrix deposition to mechanical load. On the basis of the present findings, it may be hypothesized that Ang II-induced and ET-1-induced collagen accumulation in the right ventricle might limit myocyte ability to sense the mechanical load, leading to reduced IGF-I expression and impaired ventricular performance.

References

1. Neri Serneri GG, Modesti PA, Boddi M, Cecioni I, Panicia R, Coppo M, Galanti G, Simonetti I, Vanni S, Papa L, Bandinelli B, Migliorini A, Modesti A, Maccherini M, Sani G, Toscano M. Cardiac growth factors in human hypertrophy: relations with myocardial contractility and wall stress. *Circ Res.* 1999;85:57–67.
2. Wahlander H, Wickman A, Isgaard J, Friberg P. Interaction between the renin-angiotensin system and insulin-like growth factor I in aorto-caval fistula-induced cardiac hypertrophy in rats. *Acta Physiol Scand.* 1999; 165:143–154.
3. Modesti PA, Vanni S, Bertolozzi I, Cecioni I, Polidori G, Panicia R, Bandinelli B, Perna A, Liguori P, Boddi M, Galanti G, Neri Serneri GG. Early sequence of cardiac adaptations and growth factor formation in pressure- and volume-overload hypertrophy. *Am J Physiol.* 2000;279: H976–H985.
4. Modesti PA, Zecchi-Orlandini S, Vanni S, Polidori G, Bertolozzi I, Perna AM, Formigli L, Cecioni I, Coppo M, Boddi M, Neri Serneri GG. Release of preformed Ang II from myocytes mediates angiotensinogen and ET-1 gene overexpression in vivo via AT1 receptor. *J Mol Cell Cardiol.* 2002;34:1491–1500.
5. Komuro I, Yazaki Y. Control of cardiac gene expression by mechanical stress. *Annu Rev Physiol.* 1993;55:55–75.
6. Sugden PH. Mechanotransduction in cardiomyocyte hypertrophy. *Circulation.* 2001;103:1375–1377.
7. Weber KT, Sun Y, Tyagi SC, Cleutjens JP. Collagen network of the myocardium: function, structural remodeling and regulatory mechanisms. *J Mol Cell Cardiol.* 1994;26:279–292.
8. Jalil JE, Doering CW, Janicki JS, Pick R, Shroff SG, Weber KT. Fibrillar collagen and myocardial stiffness in the intact hypertrophied rat left ventricle. *Circ Res.* 1989;64:1041–1050.
9. Namba T, Tsutsui H, Tagawa H, Takahashi M, Saito K, Kozai T, Usui M, Imanaka-Yoshida K, Imaizumi T, Takeshita A. Regulation of fibrillar collagen gene expression and protein accumulation in volume-overloaded cardiac hypertrophy. *Circulation.* 1997;95:2448–2454.
10. Dolgilevich SM, Siri FM, Atlas SA, Eng C. Changes in collagenase and collagen gene expression after induction of aortocaval fistula in rats. *Am J Physiol.* 2001;281:H207–H214.
11. Neri Serneri GG, Boddi M, Cecioni I, Vanni S, Coppo M, Papa ML, Bandinelli B, Bertolozzi I, Polidori G, Toscano T, Maccherini M, Modesti PA. Cardiac angiotensin II formation in the clinical course of heart failure and its relationship with left ventricular function. *Circ Res.* 2001;88: 961–968.
12. Liu Z, Hilbelink DR, Crockett WB, Gerdes AM. Regional changes in hemodynamics and cardiac myocyte size in rats with aortocaval fistulas. I. Developing and established hypertrophy. *Circ Res.* 1991;69:52–58.

13. Liu Z, Hilbelink DR, Gerdes AM. Regional changes in hemodynamics and cardiac myocyte size in rats with aortocaval fistulas. II. Long-term effects. *Circ Res*. 1991;69:59–65.
14. Gerdes AM, Clark LC, Capasso JM. Regression of cardiac hypertrophy after closing an aortocaval fistula in rats. *Am J Physiol*. 1995;268:H2345–H2351.
15. Ruzicka M, Keeley FW, Leenen FH. The renin-angiotensin system and volume overload-induced changes in cardiac collagen and elastin. *Circulation*. 1994;90:1989–1996.
16. Magid NM, Opio G, Wallerson DC, Young MS, Borer JS. Heart failure due to chronic experimental aortic regurgitation. *Am J Physiol*. 1994;267:H556–H562.
17. Brower GL, Henegar JR, Janicki JS. Temporal evaluation of left ventricular remodeling and function in rats with chronic volume overload. *Am J Physiol*. 1996;271:H2071–H2078.
18. Calderone A, Takahashi N, Izzo NJ Jr, Thaik CM, Colucci WS. Pressure- and volume-induced left ventricular hypertrophies are associated with distinct myocyte phenotypes and differential induction of peptide growth factor mRNAs. *Circulation*. 1995;92:2385–2390.
19. Ruzicka M, Yuan B, Leenen FH. Effects of enalapril versus losartan on regression of volume overload-induced cardiac hypertrophy in rats. *Circulation*. 1994;90:484–491.
20. Newman WH. Contractile state of hypertrophied left ventricle in long-standing volume overload. *Am J Physiol*. 1978;234:H88–H93.
21. Sahn DJ, DeMaria A, Kisslo J, Weyman A. The Committee on M-mode standardization of the American Society of Echocardiography: recommendations regarding quantitation in M-mode echocardiography: results of a survey of echocardiographic measurements. *Circulation*. 1978;58:1072–1083.
22. Kavarana MN, Pessin-Minsley MS, Urtecho J, Catanese KA, Flannery M, Oz MC, Naka Y. Right ventricular dysfunction and organ failure in left ventricular assist device recipients: a continuing problem. *Ann Thorac Surg*. 2002;73:745–750.
23. Wei CM, Lerman A, Rodeheffer RJ, McGregor CG, Brandt RR, Wright S, Heublein DM, Kao PC, Edwards WD, Burnett JC Jr. Endothelin in human congestive heart failure. *Circulation*. 1994;89:1580–1586.
24. Jalil JE, Ebensperger R, Melendez J, Acevedo E, Sapag-Hagar M, Gonzalez-Jara F, Galvez A, Perez-Montes V, Lavandro S. Effects of antihypertensive treatment on cardiac IGF-I during prevention of ventricular hypertrophy in the rat. *Life Sci*. 1999;64:1603–1612.
25. Woessner JF. The determination of hydroxyproline in tissue and protein samples containing small proportions of this amino acid. *Arch Biochem Biophys*. 1961;93:440–447.
26. Tamura T, Onodera T, Said S, Gerdes AM. Correlation of myocyte lengthening to chamber dilation in the spontaneously hypertensive heart failure (SHHF) rat. *J Mol Cell Cardiol*. 1998;30:2175–2181.
27. Mercadier JJ, Lompre AM, Wisnewsky C, Samuel JL, Bercovici J, Swynghedauw B, Schwartz K. Myosin isoenzyme changes in several models of rat cardiac hypertrophy. *Circ Res*. 1981;49:525–532.
28. Legault F, Rouleau JL, Juneau C, Rose C, Rakusan K. Functional and morphological characteristics of compensated and decompensated cardiac hypertrophy in dogs with chronic infrarenal aorto-caval fistulas. *Circ Res*. 1990;66:846–859.
29. Ross J Jr, Sonnenblick EH, Taylor RR, Spotnitz HM, Covell JW. Diastolic geometry and sarcomere lengths in the chronically dilated canine left ventricle. *Circ Res*. 1971;28:49–61.
30. Carabello BA, Zile MR, Tanaka R, Cooper G 4th. Left ventricular hypertrophy due to volume overload versus pressure overload. *Am J Physiol*. 1992;263:H1137–H1144.
31. Carabello BA, Nolan SP, McGuire LB. Assessment of preoperative left ventricular function in patients with mitral regurgitation: value of the end-systolic wall stress-end-systolic volume ratio. *Circulation*. 1981;64:1212–1217.
32. Ishibashi Y, Rembert JC, Carabello BA, Nemoto S, Hamawaki M, Zile MR, Greenfield JC Jr, Cooper G IV. Normal myocardial function in severe right ventricular volume overload hypertrophy. *Am J Physiol*. 2001;280:H11–H16.
33. Neri Serneri GG, Boddi M, Modesti PA, Cecioni I, Coppo M, Padeletti L, Michelucci A, Colella A, Galanti G. Increased cardiac sympathetic activity and insulin-like growth factor-I formation are associated with physiological hypertrophy in athletes. *Circ Res*. 2001;89:977–982.
34. McKoy G, Ashley W, Mander J, Yang SY, Williams N, Russell B, Goldspink G. Expression of insulin growth factor-1 splice variants and structural genes in rabbit skeletal muscle induced by stretch and stimulation. *J Physiol*. 1999;516:583–592.
35. Ito H, Hiroe M, Hirata Y, Tsujino M, Adachi S, Shichiri M, Koike A, Nogami A, Marumo F. Insulin-like growth factor-I induces hypertrophy with enhanced expression of muscle specific genes in cultured rat cardiomyocytes. *Circulation*. 1993;87:1715–1721.
36. Eble DM, Strait JB, Govindarajan G, Lou J, Byron KL, Samarel AM. Endothelin-induced cardiac myocyte hypertrophy: role for focal adhesion kinase. *Am J Physiol*. 2000;278:H1695–H1707.
37. Oka T, Nishimura H, Ueyama M, Kubota J, Kawamura K. Lisinopril reduces cardiac hypertrophy and mortality in rats with aortocaval fistula. *Eur J Pharmacol*. 1993;234:55–60.
38. Dell'italia LJ, Balcells E, Meng QC, Su X, Schultz D, Bishop SP, Machida N, Straeter-Knowlen IM, Hankes GH, Dillon R, Cartee RE, Oparil S. Volume-overload cardiac hypertrophy is unaffected by ACE inhibitor treatment in dogs. *Am J Physiol*. 1997;273:H961–H970.
39. Peters TH, Sharma HS, Yilmaz E, Bogers AJ. Quantitative analysis of collagens and fibronectin expression in human right ventricular hypertrophy. *Ann N Y Acad Sci*. 1999;874:278–285.
40. Hafizi S, Wharton J, Morgan K, Allen SP, Chester AH, Catravas JD, Polak JM, Yacoub MH. Expression of functional angiotensin-converting enzyme and AT1 receptors in cultured human cardiac fibroblasts. *Circulation*. 1998;98:2553–2559.
41. Kawano H, Do YS, Kawano Y, Starnes V, Barr M, Law RE, Hsueh WA. Angiotensin II has multiple profibrotic effects in human cardiac fibroblasts. *Circulation*. 2000;101:1130–1137.
42. Matsubara H. Pathophysiological role of angiotensin II type 2 receptor in cardiovascular and renal diseases. *Circ Res*. 1998;83:1182–1191.
43. Kim NN, Villegas S, Summerour SR, Villarreal FJ. Regulation of cardiac fibroblast extracellular matrix production by bradykinin and nitric oxide. *J Mol Cell Cardiol*. 1999;31:457–466.
44. Liu YH, Yang XP, Sharov VG, Nass O, Sabbah HN, Peterson E, Carretero OA. Effects of angiotensin-converting enzyme inhibitors and angiotensin II type 1 receptor antagonists in rats with heart failure: role of kinins and angiotensin II type 2 receptors. *J Clin Invest*. 1997;99:1926–1935.
45. Akazawa H, Komuro I. Roles of cardiac transcription factors in cardiac hypertrophy. *Circ Res*. 2003;92:1079–1088.
46. Hautala N, Tenhunen O, Szokodi I, Ruskoaho H. Direct left ventricular wall stretch activates GATA4 binding in perfused rat heart: involvement of autocrine/paracrine pathways. *Pflugers Arch*. 2002;443:362–369.
47. Bamman MM, Shipp JR, Jiang J, Gower BA, Hunter GR, Goodman A, McLafferty CL Jr, Urban RJ. Mechanical load increases muscle IGF-I and androgen receptor mRNA concentrations in humans. *Am J Physiol*. 2001;280:E383–E390.
48. Li Q, Li B, Wang X, Leri A, Jana KP, Liu Y, Kajstura J, Baserga R, Anversa P. Overexpression of insulin-like growth factor-1 in mice protects from myocyte death after infarction, attenuating ventricular dilation, wall stress, and cardiac hypertrophy. *J Clin Invest*. 1997;100:1991–1999.